Ultrabroadband operation of a femtosecond optical parametric generator based on BiB_3O_6 in the near-IR

Alexander Gaydardzhiev,[1] Ivaylo Nikolov,[1] Ivan Buchvarov,[1] Valentin Petrov,[2*] and Frank Noack[2]

[1]*Department of Physics, Sofia University, 5 James Bourchier Blvd., BG-1164 Sofia, Bulgaria*
[2]*Max-Born-Institute for Nonlinear Optics and Ultrafast Spectroscopy, 2A Max-Born-Str. D-12489 Berlin, Germany*
**Corresponding author: petrov@mbi-berlin.de*

Abstract: Ultrabroadband optical parametric generation in the near-IR (~135 THz, 1.15-2.4 μm) is demonstrated using bismuth triborate, BiB_3O_6 (BIBO), in a collinear geometry. The white light continuum energy obtained with a single stage reached 15 μJ (internal conversion efficiency of ≈7%). Integral pulse durations as short as 63 fs were derived from the recorded FROG traces, comparable to the 45 fs pulse duration of the 1 kHz Ti:sapphire regenerative amplifier used for pumping at 800 nm.

OCIS codes: (190.4970) Parametric oscillators and amplifiers; (190.4400) Nonlinear optics, materials; (190.7110) Ultrafast nonlinear optics.

References and links

1. R. Danielius, A. Piskarskas, A. Stabinis, G. P. Banfi, P. Di Trapani, and R. Righini, "Traveling-wave parametric generation of widely tunable, highly coherent femtosecond light pulses," J. Opt. Soc. Am. **10**, 2222-2232 (1993).
2. G. Cerullo and S. De Silvestri, "Ultrafast optical parametric amplifiers," Rev. Sci. Instrum. **74**, 1-18 (2003).
3. A. Brodeur and S. L. Chin, "Ultrafast white-light continuum generation and self-focusing in transparent condensed media," J. Opt. Soc. Am. B **16**, 637-650 (1999).
4. I. Nikolov, A. Gaydardzhiev, I. Buchvarov, P. Tzankov, F. Noack, and V. Petrov, "Ultrabroadband continuum amplification in the near infrared using BiB_3O_6 nonlinear crystals pumped at 800 nm," Opt. Lett. **32**, 3342-3344 (2007).
5. H. Hellwig, J. Liebertz, and L. Bohaty, "Exceptional large nonlinear optical coefficients in the monoclinic bismuth borate BiB_3O_6 (BIBO)," Solid State Commun. **109**, 249-251 (1999).
6. A. Birmontas, A. Piskarskas, and A. Stabinis, "Dispersion anomalies of tuning characteristics and spectrum of an optical parametric oscillator," Sov. J. Quantum Electron. **13**, 1243-1246 (1983) [transl. from Kvantovaya Elektron. (Moscow) **10**, 1881-1884 (1983)].
7. N. Umemura, K. Miyata, and K. Kato, "New data on the optical properties of BiB_3O_6," Opt. Mater. **30**, 532-534 (2007).
8. X. Liu, D. Deng, M. Li, D. Guo, and Z. Xu, "Retracing behaviour of the phase-matching angle of nonlinear crystals in optical parametric oscillators," J. Appl. Phys. **74**, 2989-2991 (1993).
9. V. Petrov, F. Noack, P. Tzankov, M. Ghotbi, M. Ebrahim-Zadeh, I. Nikolov, and I. Buchvarov, "High-power femtosecond optical parametric amplification at 1 kHz in BiB_3O_6 pumped at 800 nm," Opt. Express **15**, 556-563 (2007).
10. M. S. Webb, D. Eimerl, and S. P. Velsko, "Wavelength insensitive phase-matched second-harmonic generation in partially deuterated KDP," J. Opt. Soc. Am. B **9**, 1118-1127 (2007).
11. D. N. Nikogosyan, *Nonlinear Optical Crystals*, (Springer, New York, 2005).
12. B. Bareika, A. Birmontas, G. Dikchyus, A. Piskarskas, V. Sirutkaitis, and A. Stabinis, "Parametric generation of picosecond continuum in near-infrared and visible ranges on the basis of a quadratic nonlinearity," Sov. J. Quantum Electron. **12**, 1654-1656 (1982) [transl. from Kvantovaya Elektron. (Moscow) **9**, 2534-2536 (1982)].
13. M. Tiihonen, V. Pasiskevicius, A. Fragemann, C. Canalias, and F. Laurell, "Ultrabroadband gain in optical parametric generator with periodically poled $KTiOPO_4$," Appl. Phys. B **85**, 73-77 (2006).
14. S. N. Orlov, E. V. Pestryakov, and Yu. N. Polivanov, "Optical parametric amplification with bandwidth exceeding an octave," Quantum Electron. **34**, 477-479 (2004) [transl. from Kvantovaya Elektron. (Moscow) **34**, 477-481 (2004)].

#91218 - $15.00 USD Received 2 Jan 2008; revised 31 Jan 2008; accepted 31 Jan 2008; published 5 Feb 2008

1. Introduction

The availability of ultrabroadband coherent radiation in the near-IR in combination with femtosecond pulse durations could find numerous applications in various fields such as time-resolved broadband spectroscopy, spectral comb generation for metrology or high-harmonic generation. Although vibronic lasers based on the Cr^{2+}-ion show broad tunability in the 2-3 μm spectral range, optical parametric amplification provides in general much larger spectral bandwidths (exceeding an octave) than any known laser material. With the invention of the Ti:sapphire based femtosecond amplifiers operating near 800 nm at repetition rates of the order of 1 kHz and the crystals of the borate family, e.g. β-BaB_2O_4 (BBO) and LiB_3O_5 (LBO), combining high nonlinearity and damage threshold, several parametric schemes for efficient generation of femtosecond pulses in the near-IR were developed in the beginning of the 1990's. Their first stage was based either on amplification of the parametric super-fluorescence (optical parametric generator, OPG) or the amplification of white-light continuum (WLC), (optical parametric amplifier, OPA) [1,2]. It should be noted that although such WLC generation in transparent materials using a single filament [3] could find some direct applications as a source of broadband coherent radiation, typical energies produced by such schemes operating at 1 kHz are very low, of the order of 10s of nJ.

Very recently, we demonstrated ultrabroadband WLC amplification in the near-IR in crystals of bismuth borate (BiB_3O_6 or shortly BIBO) [4]. The WLC seed was generated in that case by a single filament in YAG but obviously, such an OPA can be used to amplify also the weak WLC produced in microstructured or tapered fibers. When collinear e→oo interaction in the x-z plane of the monoclinic BIBO is used, not only the group velocity mismatch (GVM) between the signal and idler waves vanishes near degeneracy (achromatic phase-matching) but, especially for pump wavelengths near 800 nm, this is accompanied by vanishing group velocity dispersion (GVD) of the signal and idler. The latter effect is not present when achromatic phase-matching is achieved by non-collinear phase-matching, a technique used when broadband operation away from degeneracy is desirable [2].

Utilizing the above mentioned properties of BIBO, it was possible to reach an amplification bandwidth extending over an octave (1.2-2.4 μm) but although energies as high as 50 μJ were obtained with a 5 mm long BIBO crystal in collinear geometry, the whole set-up was extremely complex requiring a special pump source above 2 μm for the generation of the WLC seed. In the present work we investigate a much simpler collinear OPG scheme based on a single stage of BIBO pumped near 800 nm, which produces output energies on the 10 μJ level with comparable bandwidth and shorter integral pulse duration.

2. Properties of BIBO as a broadband parametric amplifier

BIBO is particularly well suited for realization of down-converting optical parametric devices requiring high gain such as OPAs and OPGs, because of its high second order nonlinear susceptibility in relation to its bandgap. For example, for pumping near 800 nm and e→oo interaction in the x-z plane, $d_{\text{eff}}(\text{BIBO})=d_{12}\cos\theta=3.14$ pm/V at a signal wavelength of 1400 nm which is higher than that of $KTiOPO_4$ (KTP), $d_{\text{eff}}(\text{KTP})<2.65$ pm/V, see [5]. Comparing with other borate materials, it is clear that similar parametric gain can be achieved with a thinner crystal of BIBO permitting larger amplification bandwidths. However, the main and unique advantages of this material for femtosecond OPA/OPG applications are related to its dispersive properties. That is why these properties will be considered below in more detail.

In the plane-wave approximation, in the absence of pump depletion, the steady state gain for the signal wave (intensity) is given by [1,2]:

$$G = 1 + \frac{\Gamma^2}{g^2}\sinh^2(gL) \tag{1}$$

#91218 - $15.00 USD Received 2 Jan 2008; revised 31 Jan 2008; accepted 31 Jan 2008; published 5 Feb 2008

with $g = \sqrt{\Gamma^2 - (\Delta k/2)^2}$ where $\Delta k = k_S + k_I - k_P$ is the wave mismatch and the exponential gain coefficient Γ is defined by $\Gamma^2 = \frac{8\pi^2 d_{eff}^2 I_P}{n_P n_S n_I \lambda_I \lambda_S \varepsilon_0 c}$. In the large gain ($\Gamma L >> 1$) limit the above equation simplifies to:

$$G = \frac{1}{4} exp(2gL) \tag{2}$$

In order to obtain analytical expressions for the parametric gain bandwidth, the wave mismatch is usually expanded in series as a function of the frequency, assuming in a first approximation that the pump is monochromatic,

$$\begin{aligned} \Delta k = \Delta k_0 + \left(\frac{\partial k_S}{\partial \omega_S} - \frac{\partial k_I}{\partial \omega_I}\right)\Delta\omega + \frac{1}{2!}\left(\frac{\partial^2 k_S}{\partial \omega_S^2} + \frac{\partial^2 k_I}{\partial \omega_I^2}\right)(\Delta\omega)^2 + \\ + \frac{1}{3!}\left(\frac{\partial^3 k_S}{\partial \omega_S^3} - \frac{\partial^3 k_I}{\partial \omega_I^3}\right)(\Delta\omega)^3 + \frac{1}{4!}\left(\frac{\partial^4 k_S}{\partial \omega_S^4} + \frac{\partial^4 k}{\partial \omega_I^4}\right)(\Delta\omega)^4 ..... \end{aligned} \tag{3}$$

where $\Delta\omega = \Delta\omega_S$ denotes the frequency change of the signal wave and by energy conservation the idler frequency change will be $\Delta\omega_I = -\Delta\omega$. The phase-matching condition means that $\Delta k_0 = 0$. The individual terms in (3) are used to evaluate the points, in terms of frequency, where the gain function G from Eq. (2) drops to 50% of its maximum value which corresponds to the wave vector mismatch $\Delta k_{1/2} \approx \pm 2(\ln 2)^{1/2}(\Gamma/L)^{1/2}$. The results when using the first derivative (GVM approximation) and the second derivative (GVD approximation) are well known [1,2] and read, in terms of FWHM for $\Delta\nu = \Delta\omega/2\pi$:

$$\Delta\nu = \frac{2(ln2)^{1/2}}{\pi}\left(\frac{\Gamma}{L}\right)^{1/2}\left|\frac{1}{v_S} - \frac{1}{v_I}\right|^{-1} \tag{4}$$

$$\Delta\nu = \frac{2(ln2)^{1/4}}{\pi}\left(\frac{\Gamma}{L}\right)^{1/4}\left|\frac{\partial^2 k_S}{\partial \omega_S^2} + \frac{\partial^2 k_I}{\partial \omega_I^2}\right|^{-1/2} \tag{5}$$

Considering the next terms one obtains from Eqs. (2) and (3):

$$\Delta\nu = \frac{(144 ln2)^{1/6}}{\pi}\left(\frac{\Gamma}{L}\right)^{1/6}\left|\frac{\partial^3 k_S}{\partial \omega_S^3} - \frac{\partial^3 k_I}{\partial \omega_I^3}\right|^{-1/3} \tag{6}$$

$$\Delta\nu = \frac{2(9 ln2)^{1/8}}{\pi}\left(\frac{\Gamma}{L}\right)^{1/8}\left|\frac{\partial^4 k_S}{\partial \omega_S^4} + \frac{\partial^4 k_I}{\partial \omega_I^4}\right|^{-1/4} \tag{7}$$

#91218 - $15.00 USD Received 2 Jan 2008; revised 31 Jan 2008; accepted 31 Jan 2008; published 5 Feb 2008

It is clear that for collinear type-I interaction the third order term, Eq. (6), also vanishes near degeneracy and this makes it necessary to consider the fourth order term [6]. From our consideration, this term is given by Eq. (7). From the four approximations, one should use, depending on the signal wavelength, the one which predicts the smallest gain bandwidth. In the λ_S=1100-1300 nm range, for e→oo interaction in the x-z plane of BIBO pumped at 800 nm, this is the solution based on the GVM term. Approaching degeneracy, however, the GVD term also vanishes which is a consequence of the fact that for polarization parallel to the y-axis (o-wave for the present interaction scheme), it is zero at 1580 nm.

It is interesting that the fourth order approximation should be used for BIBO starting already from 1500 nm, see Fig. 1. This approximation predicts a gain bandwidth (FWHM intensity) of about 3800 cm^{-1} (116 THz) near degeneracy. The Sellmeier equations used in the calculation for BIBO were those recently refined [7]. In contrast, the spectral bandwidth of BBO for the same crystal and pump parameters is determined near degeneracy by the second order derivatives and amounts to 63 THz, i.e. it is roughly two times smaller, see Fig. 1.

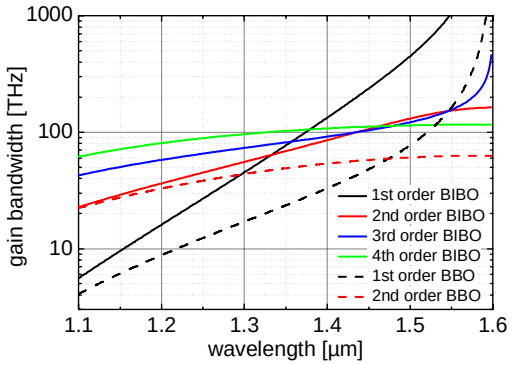

Fig. 1. Gain bandwidth (FWHM) of BIBO and BBO, analytically calculated for collinear type e→oo interaction at λ_P=800 nm, a crystal length of 5 mm and pump intensity of 50 GW/cm^2 using only the first, second, third and fourth order Taylor series expansion terms of the wave-vector mismatch Δk, respectively.

Direct calculations of the parametric gain G using Eq. (1) at the exact phase-matching angle are presented in Fig. 2(a). In can be seen that the gain bandwidth at first increases but then decreases with the pump wavelength. There exists an optimum pump wavelength near λ_P=780 nm where the gain bandwidth is maximized, as can be seen in Fig. 2(b) where the gray area depicts the range limited by the ½ drop of the gain from its maximum value. The left part of the figure corresponds to the retracing behavior of the phase-matching curves, see Fig. 2(c), where "satellites" appear in Fig. 2(a), corresponding to the second pair of signal and idler waves phase-matched at the same angle θ.

Thus, collinear e→oo interaction in BIBO possesses for pump wavelengths near 800 nm the exclusive property of simultaneous vanishing of the first three terms that determine the gain bandwidth. Many other nonlinear crystals with sufficient birefringence possess in fact the same property provided the three wavelengths lie within the transparency range. This is related to the existence of retracing behavior of the phase-matching curves [6,8] which can be traced back to the material dispersive properties. In any case, it happens at a certain pump wavelength which does not necessarily coincide with the wavelengths of the available femtosecond sources that can be used for pumping an OPA or OPG. As can be seen from Table 1 this same property is characteristic also of periodically poled materials (Type-0 interaction) where quasi-phase-matching is realized by suitable choice of the period. Note that retracing behavior (and the gain bandwidth) can be controlled also by changing the crystal temperature, see the computed curves in Fig. 2(c).

#91218 - $15.00 USD Received 2 Jan 2008; revised 31 Jan 2008; accepted 31 Jan 2008; published 5 Feb 2008

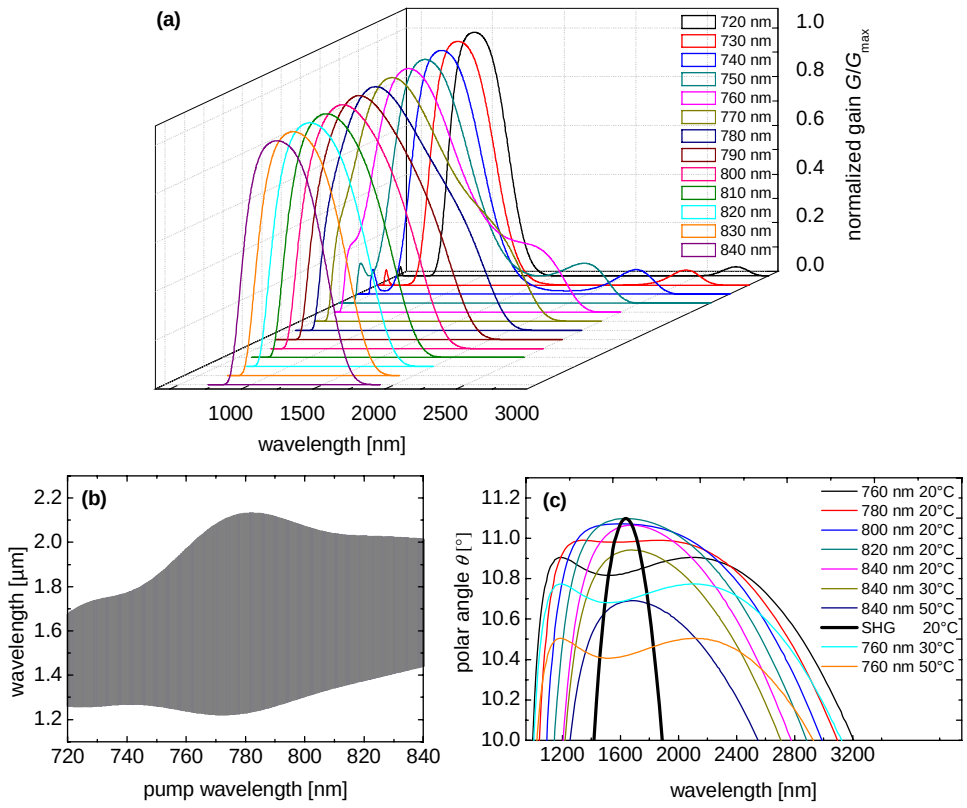

Fig. 2. (a). Normalized parametric gain in BIBO (negative type-I e→oo interaction in the x-z plane) for different pump wavelengths (indicated) at exact phase-matching angles, for a crystal length of 5 mm and pump intensity of 50 GW/cm^2, (b) gain bandwidth (FWHM) as estimated from (a), (c) phase-matching curves at different pump wavelengths and crystal temperatures (indicated) for the same process and SHG type-I (oo→e) at room temperature. The absolute gain G for (a) decreases from 1.41×10^8 at λ_P=720 nm to 2.91×10^7 at λ_P=780 nm and to 5.56×10^6 at λ_P=840 nm.

Moreover, there is another favourable property related to the dispersion characteristics of BIBO which directly affects the interaction length with the pump and consequently the achievable conversion efficiency. The retracing behavior occurs at angles for which the phase-matching curves reverse their curvature as a function of the pump wavelength, see Fig. 2(c) and [9]. The critical angle for which this happens in type-I (e→oo) BIBO is in the vicinity of the phase-matching curve turning point for the inverse process, second harmonic generation (SHG). Such a turning point (at λ_F) in the dependence of the fundamental wavelength on the phase-matching angle in SHG means nothing but broadband phase-matching which is equivalent to vanishing GVM between the fundamental and the second harmonic. Indeed, it can be easily shown that this GVM vanishes at the point where $(\partial\theta/\partial\lambda)_{\lambda_F}=0$ for the SHG phase-matching curve [10], see Fig. 2(c). The existence of a turning point in the SHG phase-matching curve, attributed to anomalous dispersion [10], determines in fact the existence of the retracing phenomenon in the OPA/OPG curves, which can be characterized by three or more turning points [8]. This can be easily seen from Fig. 2(c) but the origin of the phenomenon can be traced back to the refractive index dependences, shown for BIBO in Fig. 3.

Although similar analytical relations cannot be derived for the GVM with the pump in the case of three waves (because both the signal and idler are broadband), it is clear than an OPA/OPG operating in the vicinity of the phase-matching angle where the SHG phase-

#91218 - $15.00 USD Received 2 Jan 2008; revised 31 Jan 2008; accepted 31 Jan 2008; published 5 Feb 2008

matching curve has a turning point will be also characterized by very low GVM between the pump and the other two waves. For example, for the considered type of interaction in BIBO, the turning point of the SHG phase-matching curve occurs at a fundamental wavelength of λ_F=1637 nm. Both this wavelength and the "magic" pump wavelength for ultrabroadband parametric amplification were calculated and are presented in Table 1 for several crystals applicable in the near-IR.

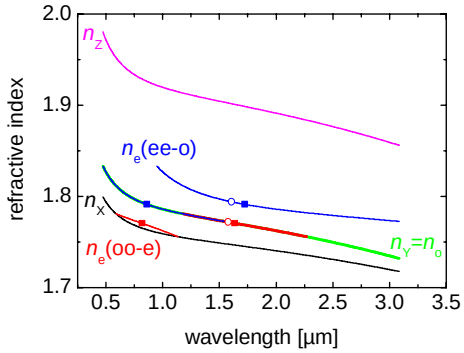

Fig. 3. Refractive index of BIBO for type-I SHG in the x-z plane. The wavelength ranges are determined by the validity of the Sellmeier expansions used (474-3083 nm) [7]. Red curves correspond to oo→e and blue curves to ee→o phase-matching. The squares indicate the points where the first derivatives of the refractive index for the fundamental and second harmonic are equal (broadband SHG phase-matching corresponding to λ_F in Table 1) and the circles indicate the points of vanishing second derivative (corresponding to twice the "magic" pump wavelength or $2\lambda_P$ in Table 1).

Table 1. Parameters of several crystals that can be used in ultrabroadband OPA/OPG schemes pumped below 1 μm: λ_P is the "magic" pump wavelength for which the signal/idler GVD vanishes near degeneracy; λ_F is the fundamental wavelength for broadband SHG, $\Delta\lambda/\Delta\nu$ correspond to the wavelength / frequency range for maximum gain bandwidth calculated at the 1/2 level (crystal length 5 mm, pump intensity 50 GW/cm^2), θ/φ and Λ are the phase-matching angle and the period for degenerate operation at the given λ_P in birefringent and quasi phase-matching, respectively, and the GVM parameter $1/v_P$-$1/v_{S,I}$ is calculated for degenerate operation at λ_P.*

Crystal	λ_P [μm]	λ_F [μm]	$\Delta\lambda$ [μm]	$\Delta\nu$ [THz]	θ/φ [°] or Λ [μm]	$1/v_P$-$1/v_{S,I}$ [fs/mm]
KDP (e→oo)	0.492	1.035	0.818-1.233	366-243	41.3	94.5
PPSLT (e→ee)	0.561	1.660	0.966-1.338	311-224	9.1	577
LBO (e→oo) x-y	0.599	1.260	0.944-1.625	317-184	3.1	18.6
CLBO (e→oo)	0.629	1.339	0.995-1.710	310-175	27.7	9.94
BBO (e→oo)	0.716	1.547	1.121-1.982	267-151	19.95	15.0
BIBO (e→oo) x-z	0.790	1.637	1.228-2.139	244-140	11.05	11.4
BIBO (o→ee) x-z	0.805	1.723	1.275-2.184	235-137	35.4	31.6
PPKTP (e→ee)	0.894	2.505	1.511-2.188	198-137	32.4	141
$LiNbO_3$ (e→oo)	0.949	2.025	1.690-2.166	177-138	45.3	36.7
PPLN (e→ee)	0.956	2.686	1.705-2.176	176-137	27.9	165
$LiIO_3$ (e→oo)	0.970	2.231	1.609-2.940	186-102	18.7	31.5
$KNbO_3$ (e→oo) x-y	0.988	2.137	1.629-2.511	184-119	47.71	46.3
$KNbO_3$ (e→oo) y-z	1.004	2.066	1.656-2.550	181-117	15.63	17.5

*The Sellmeier and nonlinear coefficient data used for the table, with the exception of BIBO, is from [11]: For KH_2PO_4 (KDP), LBO, $CsLiB_6O_{10}$ (CLBO), BBO, periodically poled KTP (PPKTP), $LiIO_3$, and $KNbO_3$, the so-called "best dispersion relations" were used; for $LiNbO_3$ and periodically poled lithium niobate (PPLN), the data chosen was for congruent material, and in the case of periodically poled stoichiometric $LiTaO_3$ (PPSLT) the data used was for stoichiometric lithium tantalate. The validity of the Sellmeier expansion does not always cover the full $\Delta\lambda$ ranges.

In the other type-I interaction scheme in BIBO the deviation of λ_F from $2\lambda_P$ is larger and consequently the GVM with the pump is also larger. In fact, Table 1 shows that the only

#91218 - $15.00 USD Received 2 Jan 2008; revised 31 Jan 2008; accepted 31 Jan 2008; published 5 Feb 2008

crystal for which the GVM with the pump at the "magic" pump wavelength is smaller than for e→oo BIBO is CLBO. Similar arguments hold also for quasi-phase-matched materials where the turning point is defined with respect to the phase-matching period. Since in this case the polarization of the three waves is the same, one can expect that the deviation of λ_F from $2\lambda_P$ should be larger, see Fig. 3, leading to larger GVM with the pump. For instance, the GVM with the pump in the degenerate PPKTP-OPA pumped at the "magic" wavelength amounts to 141 fs/mm, in PPSLT it is even 577 fs/mm while it is only 11.4 fs/mm in BIBO (e→oo).

Thus, it should be emphasized that there is nothing unique in the dispersive properties of BIBO concerning the achievable gain bandwidths, this concerns only the fact that from all existing crystals BIBO exhibits these important for ultrafast collinear OPAs/OPGs properties for a pump wavelength coinciding with the wavelength of the most widely used and technologically developed ultrafast Ti:sapphire laser amplifiers. It can be seen from Table 1 that the achievable bandwidths in the four borates considered and in KDP, exceed 100 THz. However, as a result of the specific behavior of the three refractive indices of BIBO (presumably related to anomalous infrared dispersion) the two characteristic wavelengths λ_F and $2\lambda_P$ of BIBO are very close, especially for type e→oo phase-matching, which leads to low GVM between all the three waves in a degenerate OPA/OPG pumped near 800 nm.

As already mentioned the above properties of BIBO have already been utilized by us in a femtosecond OPA configuration used to amplify WLC [4]. Generation of such a continuum using an ultrabroadband OPG (i.e. WLC based on pure quadratic nonlinearity) was demonstrated with picosecond pulses in KDP as early as 1982 [12] achieving a spectral range of 90 THz. Ultrabroadband gain extending over 115 THz was demonstrated recently also with an OPG based on PPKTP pumped by 1 ps pulses [13].

3. Experimental set-up and results

In the present experiment we studied two uncoated BIBO crystals of length 3 and 5 mm, both cut at θ=11.4° for e→oo interaction in the x-z plane (note that the o→ee polarization configuration included for completeness in Table 1 occurs in the same x-z principal plane but the effective nonlinearity for it is roughly two times lower). The samples were pumped in a single pass by a femtosecond Ti:sapphire regenerative amplifier operating near 800 nm at a repetition rate of 1 kHz. The pump intensity specified further is the average intensity (1/2 of the peak on-axis level) incident on the crystals. Behind the crystals, the residual pump radiation was blocked by a mirror transmitting the generated WLC which was then characterized by an InGaAs spectrometer and a power meter. Finally, using a fraction of the fresh pump beam (typically of the order of 100 μJ) as a gate pulse, XFROG (cross-correlation FROG based on sum-frequency generation in a 10 μm thick, type-I (oo→e) BBO crystal) measurements of the parametrically generated radiation were performed. The latter were used to reconstruct the entire spectrum and the integral pulse duration for the generated WLC as well as to obtain rough information about the phase-modulation. Collinear output was analyzed only; in the case of OPG the non-collinear geometry is undesirable because different spectral components propagate in different directions.

The pump source we used (Spectra Physics SPITFIRE) generated 45 fs pulses at 800 nm and the energy incident on the crystals was 260 μJ. Most of the measurements were performed for average pump intensities of 100 GW/cm^2 for the 3-mm thick crystal and 60 GW/cm^2 for the 5-mm thick crystal. The WLC energies, measured after blocking the pump beam, were 8 and 12 μJ for the 3- and 5-mm long BIBO crystals, respectively. It was not possible to increase further the pump intensity in the case of the thicker sample because higher order nonlinear effects were observed (non-phase-matched continuum generation). However, with the shorter crystal, it was possible to raise the pump intensity to 150 GW/cm^2 without any detrimental effects. This resulted in a total output energy of 15 μJ. Taking into account the transmission of the optics used and the Fresnel reflections at the crystal faces, this corresponds to an internal conversion efficiency of ≈7%.

#91218 - $15.00 USD Received 2 Jan 2008; revised 31 Jan 2008; accepted 31 Jan 2008; published 5 Feb 2008

Figures 4(a) and 4(b) show the measured OPG output energy for the 3 and 5-mm thick BIBO crystals, respectively, in dependence on the internal angle of the pump beam relative to the normal to the crystal surface. Increasing internal angle corresponds to decreasing phase-matching angle θ, however, direct relation is avoided here because of the inevitable inaccuracy of the crystal cut which could be of the same order as the angular changes studied. As can be expected, at some maximum phase-matching angle, in this case corresponding almost to normal incidence, there is no phase-matching and the output energy drops to zero.

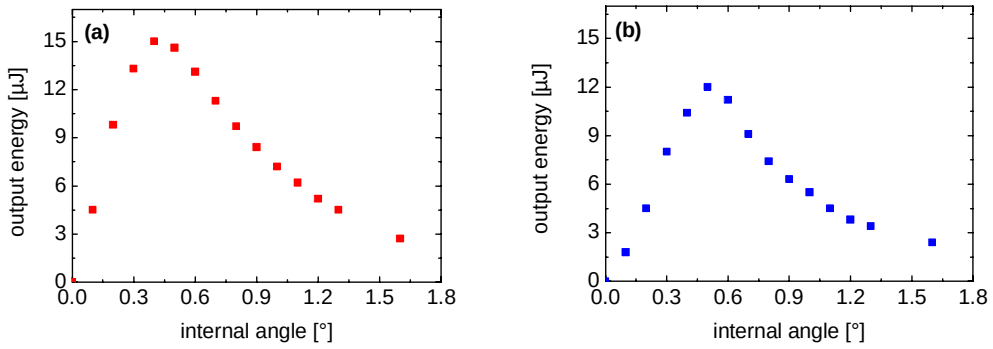

Fig. 4. OPG output energy obtained with the 3-mm (a) and 5-mm (b) thick BIBO crystals versus internal phase-matching angle relative to normal incidence. The average pump intensity (1/2 of the peak on-axis level) is 150 GW/cm^2 (a) and 60 GW/cm^2 (b).

Figures 5(a) and 5(b) show the measured OPG spectra for the 3 and 5-mm thick BIBO crystals, respectively. The dependence of the output spectra on the internal angle is in agreement with the theoretical predictions for the parametric gain shown in Figs. 6(a) and 6(b), which were calculated directly from Eq. (1). While the calculations for Fig. 2 and Table 1 were at exact phase-matching angle or period, here the phase-matching angle was varied for a fixed pump wavelength of λ_P=800 nm. In contrast to the analytical approximation used in Fig. 1, where the bandwidth is calculated only for the one wave assuming single peaked gain function, it can be seen from Fig. 6 that the actual gain bandwidth can be further increased when the spectral gain profiles for the signal and idler waves merge. Note that the phase-matching angle for which this happens is slightly lower than the one corresponding to degeneracy (θ=11.05° for λ_P=800 nm). The broadest parametric gain occurs before the two spectra have totally merged. It extends roughly from 1.2 to 2.4 μm. The additional enhancement of the bandwidth achieved in this way is up to ≈50% if compared to the values given in THz in Table 1. In fact the broadest parametric gain (depending on its definition, i.e. the acceptable dips in the spectral distribution) does not necessarily occur for the magic pump wavelength: both the pump wavelength and the phase-matching angle can slightly deviate near the values specified in Table 1, to achieve maximum bandwidths [13,14].

With increasing angle in Fig. 5, the spectra gain in bandwidth, with the broadest spectrum at an angle of ≈0.4°, corresponding to broadest parametric gain. With further increase of the angle (decrease of the phase-matching angle θ) the spectra tend to be narrower again, as can be expected for a phase-matching angle deviating from the one corresponding to degeneracy. The main qualitative difference in the spectra obtained with the 3- and 5-mm long BIBO samples is the decreasing intensity above 1500 nm, observed only for the longer crystal. For the thinner crystal, the spectral intensity remains almost constant above 1500 nm up to the limit of detection of the InGaAs array. The spectral extension of the WLC is slightly larger for the 5-mm long BIBO crystal which can be attributed to the increasing role of the GVM with the pump pulse, leading to chirp formation, as will be seen in the XFROG traces. However, having in mind the roughly 200 times higher gain in Fig. 6(b) in comparison to Fig. 6(a), it can be concluded that in the spectral range where the gain bandwidth is determined by higher order dispersion terms the effect of the gain coefficient Γ on it is rather weak [6,12].

#91218 - $15.00 USD Received 2 Jan 2008; revised 31 Jan 2008; accepted 31 Jan 2008; published 5 Feb 2008

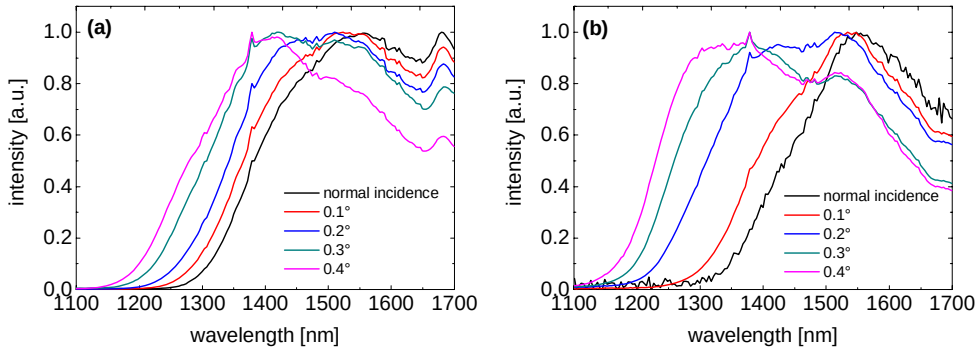

Fig. 5. OPG spectra obtained with the 3-mm (a) and 5-mm (b) thick BIBO crystals, recorded with an InGaAs spectrometer at five different internal angles of the pump beam. The pump intensity is 100 GW/cm^2 (a) and 60 GW/cm^2 (b).

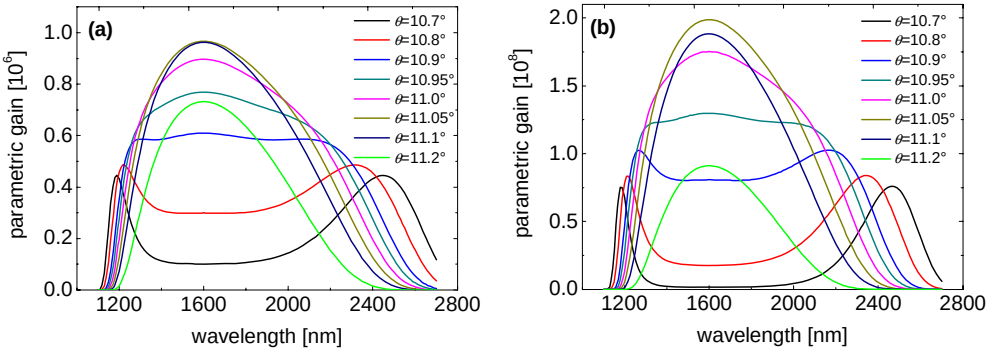

Fig. 6. Parametric gain of BIBO for collinear type e→oo interaction at λ_P=800 nm, calculated for several fixed phase-matching angles close to degeneracy (θ=11.05°). The crystal length, 3 mm (a) and 5 mm (b), and the pump intensity, 100 GW/cm^2 (a) and 60 GW/cm^2 (b), correspond to the experimental conditions in Fig. 5.

Figures 7-9 show the output spectra (a), the XFROG traces (b) and the cross-correlation functions with the gate pulse obtained by integration of the XFROG traces (c) for these three cases. The spectral portions up to 1600 nm shown by the red curves in Figs. 7(a)-9(a) are from direct measurements with the InGaAs spectrometer. The black curves in the same figures show the spectra which were reconstructed from the XFROG traces recorded with a VIS spectrometer. Finally, the parts of the amplified spectra above 1600 nm, shown by blue lines in Figs. 7(a)-9(a), were calculated using the Manley-Rowe relation. In all three cases the correspondence between the two methods used to recover the spectral information is rather satisfactory. Taking as a measure the spectra derived from the XFROG traces, the spectral extension of the generated WLC at the 0-level is roughly 135 THz in all the three cases.

As can be seen from Figs. 7(c)-9(c), the integrated cross correlation functions are well fitted by Gaussian curves. Since the autocorrelation function of the pump pulses was also analyzed using such a pulse shape, we deconvolved the cross-correlation traces under the same assumption. The resulting integral WLC pulse durations are indicated in the figures as FWHM intensity τ. The obtained pulse durations are shorter than in the OPA case [4]. The shortest pulse duration, τ=63 fs, was measured for the case of the 3-mm long crystal pumped at 100 GW/cm^2. As can be expected this occurs at the lowest conversion efficiency. The calculated time-bandwidth products are roughly 10 times above the Fourier limit for Gaussian pulse shapes: $\Delta\nu\tau\approx$4.2 for Fig. 7, ≈4.7 for Fig. 8, and ≈5 for Fig. 9.

The shape of the XFROG traces in Figs. 7(b)-9(b) is similar to the one obtained in our analogous OPA experiments [4]. In principle, this result confirms our estimations that the phase-modulation observed at the OPA output is not caused by the WLC generator or some

#91218 - $15.00 USD Received 2 Jan 2008; revised 31 Jan 2008; accepted 31 Jan 2008; published 5 Feb 2008

passive optical elements but is rather due to the BIBO crystal itself. The same can be obviously expected in the OPG case. Since the zero GVD point is very close to the point separating the signal and idler branch, opposite chirp is observed in the two branches, Fig. 10. On the other hand, opposite sign of the chirp is anyway a condition imposed by the energy conservation law in three-wave interactions, at least under the assumptions stated in section 2.

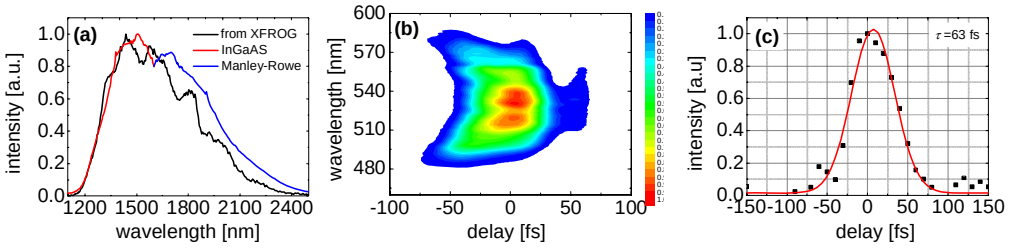

Fig. 7. Spectrum (a), XFROG trace (b) and cross-correlation function with Gaussian fit (c) of the OPG output with the 3-mm thick BIBO crystal; pump intensity: 100 GW/cm^2.

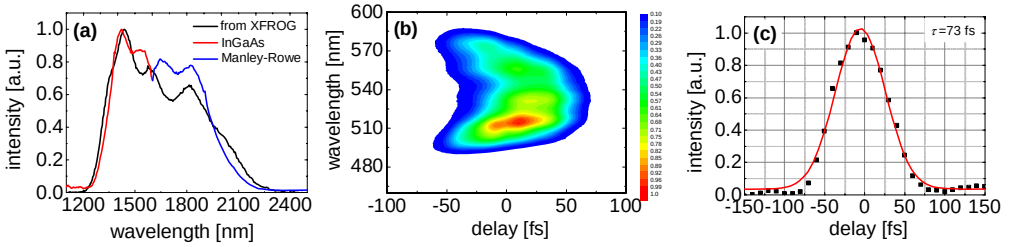

Fig. 8. Spectrum (a), XFROG trace (b) and cross-correlation function with Gaussian fit (c) of the OPG output with the 5-mm thick BIBO crystal; pump intensity: 60 GW/cm^2.

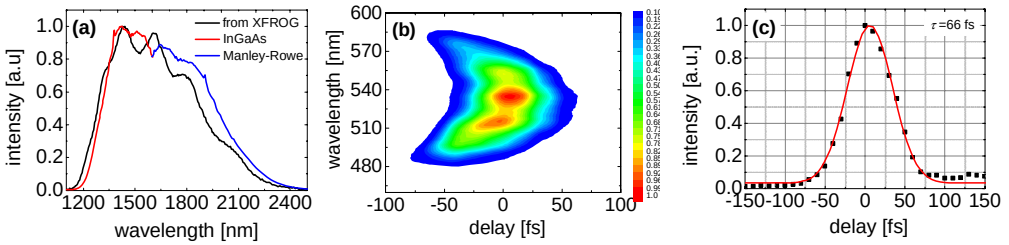

Fig. 9. Spectrum (a), XFROG trace (b) and cross-correlation function with Gaussian fit (c) of the OPG output with the 3-mm thick BIBO crystal; pump intensity: 150 GW/cm^2.

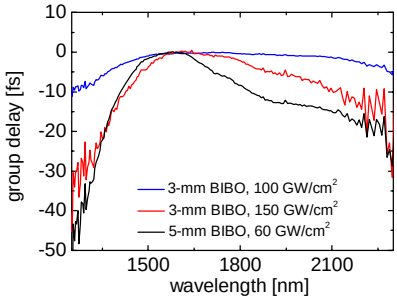

Fig. 10. Group delay derived from the XFROG traces for the three cases depicted in Figs. 7-9.

Two main conclusions can be drawn from the shape of the XFROG traces and the chirp behavior: (i) The fact that the zero GVD point separates the signal and idler spectral ranges is

#91218 - $15.00 USD Received 2 Jan 2008; revised 31 Jan 2008; accepted 31 Jan 2008; published 5 Feb 2008

not favorable for amplification of linearly chirped WLC with subsequent compression because normally the BIBO crystal itself (the material with the smallest band-gap if compared to the transfer optics and the WLC generator) is the main source of chirp. Hence, the generation of few cycle pulses, as supported from the observed bandwidths cannot profit from the amplification of WLC [4], the situation in a BIBO based OPG as the one investigated in the present work is similar. (ii) Compression of the output pulses in order to reduce the time-bandwidth product and obtain few cycle pulses should be in principle possible but will require more sophisticated schemes than a simple prism or grating compressor. Chirped mirrors could be one alternative. However, spectral selection of the signal or idler branch from the OPG spectra could be feasible to produce sub-20 fs pulses with microjoule energy using a simple compressor to compensate the quadratic phase term.

Finally, we performed an additional series of experiments to establish the effect of the pump pulse duration on the OPG performance. An analogous pump source at 800 nm delivering pulses of 100 fs duration was employed. Typical pump energies incident on the crystals were 300 μJ. At similar pump intensities the energy output from both, the 3-mm thick and the 5-mm thick BIBO crystals was doubled. In terms of spectral bandwidth, pulse duration, and time-bandwidth products, the results were similar to those described above. The integral pulse durations in this case were shorter than the pump pulses and the chirp was not pronounced.

In conclusion, we have demonstrated ultrabroadband optical parametric generation in the near-IR with WLC energy on the 10 μJ level and internal conversion efficiency as high as 7% for a single collinear stage. The spectral extension covers an octave and the pulse duration is in the sub-100 fs range. This is the first time such WLC has been generated by a second order nonlinear process on the femtosecond time scale. The presented experimental results confirm that BIBO possesses a unique combination of excellent properties for efficient conversion of femtosecond pulses from the 800 nm spectral range to the near-IR. Further investigation of the temporal modification of the WLC characteristics in the BIBO based OPG will require gate pulses with duration shorter than that of the pump pulses to be used in the XFROG analysis.

Acknowledgment

We acknowledge financial support from the German-Bulgarian exchange programme (DAAD grant D/05/11319 and Bulgarian Ministry of Science and Education grants D01-81/2006 and and D01-619/2007).

#91218 - $15.00 USD Received 2 Jan 2008; revised 31 Jan 2008; accepted 31 Jan 2008; published 5 Feb 2008